AD-A060 344 CALIFORNIA UNIV LOS ANGELES DEPT OF MECHANICS AND ST--ETC F/G 13/10.1
VIBRATION AND STABILITY ANALYSIS OF ARBITRARY STIFFENED SHELLS --ETC(U)
JUL 78 A J BRONOWICKI, R B NELSON N00014-76-C-0922
UNCLASSIFIED UCLA-ENG-7841 NL

1 OF 1
AD A060344

END
DATE FILMED
12-78
DDC

Code 474
NR 064-550

LEVEL II

Prepared for
Office of Naval Research
under Contract N00014-76-C-0922

UCLA-ENG-7841
JULY 1978

VIBRATION AND STABILITY ANALYSIS OF ARBITRARY STIFFENED SHELLS OF REVOLUTION

A. J. BRONOWICKI
R. B. NELSON

UCLA • SCHOOL OF ENGINEERING AND APPLIED SCIENCE

SECURITY CLASSIFICATION OF THIS PAGE *(When Data Entered)*

REPORT DOCUMENTATION PAGE

READ INSTRUCTIONS BEFORE COMPLETING FORM

1. REPORT NUMBER
2. GOVT ACCESSION NO.
3. RECIPIENT'S CATALOG NUMBER

4. TITLE *(and Subtitle)*

"Vibration and Stability Analysis of Arbitrary Stiffened Shells of Revolution"

5. TYPE OF REPORT & PERIOD COVERED

6. PERFORMING ORG. REPORT NUMBER

7. AUTHOR(s)

Allen J./Bronowicki
Richard B./Nelson

8. CONTRACT OR GRANT NUMBER(s)

N00014-76-C-0922

9. PERFORMING ORGANIZATION NAME AND ADDRESS

10. PROGRAM ELEMENT, PROJECT, TASK AREA & WORK UNIT NUMBERS

11. CONTROLLING OFFICE NAME AND ADDRESS

12. REPORT DATE

July 1978

13. NUMBER OF PAGES

38p.

14. MONITORING AGENCY NAME & ADDRESS *(if different from Controlling Office)*

Director, Office of Naval Research
Branch Office - Pasadena
1030 E. Green St., Pasadena, CA 91101

15. SECURITY CLASS. *(of this report)*

15a. DECLASSIFICATION/DOWNGRADING SCHEDULE

16. DISTRIBUTION STATEMENT *(of this Report)*

This document has been approved for public release and sale; its distribution is unlimited.

UCLA-ENG-7841

17. DISTRIBUTION STATEMENT *(of the abstract entered in Block 20, if different from Report)*

18. SUPPLEMENTARY NOTES

19. KEY WORDS *(Continue on reverse side if necessary and identify by block number)*

Shells of Revolution, Static, Dynamic, Buckling Analysis, Third Order Shell Theory

20. ABSTRACT *(Continue on reverse side if necessary and identify by block number)*

This report presents the analytical development of a finite element model suitable for a study of the elastic vibration and stability characteristics of a structure composed of a finite number of shells of revolution, each in the shape of a conical frustum. Thus, the model can be used to study a shell of revolution, with arbitrary meridional cross section, to which is attached arbitrarily shaped circumferential ring stiffeners and lateral bulkheads.

DD FORM 1 JAN 73 1473 EDITION OF 1 NOV 65 IS OBSOLETE
S/N 0102-LF-014-6601

SECURITY CLASSIFICATION OF THIS PAGE *(When Data Entered)*

409 458 78 10 03 003

The shell theory used to model each conical frustum is a third order Flugge-Lure-Byrne theory in which a complete interaction between shell membrane and bending effects occurs.

Energy forms are used to generate stiffness, mass and stability matrices required for the finite element. The stability functional employed is Bolotin's initial stress functional to which is appended an external potential for normal pressure loadings as defined by Cohen.

All variables used to describe the system are represented by means of Fourier series in the circumferential angle θ. Except for the stability functional, a complete decoupling exists so that only terms associated with a given circumferential mode number n interact. For the stability functional only the initial stresses associated with the symmetric pressure field are considered in order to complete the Fourier decomposition, but both initial membrane and bending stresses are retained.

The kinematical behavior of the displacement field of the conical frustum segment associated with each mode number n is defined by two different models. For the first (simpler) model, the normal (outward) displacements are third order polynomial functions of the position along the generator, while the in-surface displacement fields are first order. For the second (refined) model, the normal displacements are fifth order polynomials and the in-surface displacements are third order. Thus the simpler model of the conical frustum has two nodal planes (perpendicular to the axis of the frustum) and four degrees of freedom at each node, totalling eight degrees of freedom for the element. The refined element has three nodal planes again with four degrees of freedom at each, so that the finite element model has twelve degrees of freedom. All integrations required to generate the stiffness, mass and stability matrices, are performed numerically, using Gaussian quadrature.

The finite element models presented herein are to be basic elements in an anlysis program designed specifically for use in a program for the automated structural design of submerged stiffened pressure vessels in the form of arbitrary structures of revolution.

VIBRATION AND STABILITY ANALYSIS OF ARBITRARY STIFFENED SHELLS OF REVOLUTION

by

A.J. Bronowicki
R.B. Nelson

Prepared for
Office of Naval Research
Contract No. N00014-76-C-0922

Mechanics and Structures Department
School of Engineering and Applied Science
University of California
Los Angeles, California 90024

ABSTRACT

This report presents the analytical development of a finite element model suitable for a study of the elastic vibration and stability characteristics of a structure composed of a finite number of shells of revolution, each in the shape of a conical frustum. Thus, the model can be used to study a shell of revolution, with arbitrary meridional cross section, to which is attached arbitrarily shaped circumferential ring stiffeners and lateral bulkheads.

The shell theory used to model each conical frustum is a third order Flugge-Lure-Byrne theory in which a complete interaction between shell membrane and bending effects occurs.

Energy forms are used to generate stiffness, mass and stability matrices required for the finite element. The stability functional employed is Bolotin's initial stress functional to which is appended an external potential for normal pressure loadings as defined by Cohen.

All variables used to describe the system are represented by means of Fourier series in the circumferential angle θ. Except for the stability functional, a complete decoupling exists so that only terms associated with a given circumferential mode number n interact. For the stability functional only the initial stresses associated with the symmetric pressure field are considered in order to complete the Fourier decomposition, but both initial membrane and bending stresses are retained.

The kinematical behavior of the displacement field of the conical frustum segment associated with each mode number n is defined by two different models. For the first (simpler) model,

the normal (outward) displacements are third order polynomial functions of the position along the generator, while the in-surface displacement fields are first order. For the second (refined) model, the normal displacements are fifth order polynomials and the in-surface displacements are third order. Thus the simpler model of the conical frustum has two nodal planes (perpendicular to the axis of the frustum) and four degrees of freedom at each node, totalling eight degrees of freedom for the element. The refined element has three nodal planes again with four degrees of freedom at each, so that the finite element model has twelve degrees of freedom. All integrations required to generate the stiffness, mass and stability matrices, are performed numerically, using Gaussian quadrature.

The finite element models presented herein are to be basic elements in an analysis program designed specifically for use in a program for the automated structural design of submerged stiffened pressure vessels in the form of arbitrary structures of revolution.

I. INTRODUCTION

This report presents the analytical development of a finite element model suitable for the analysis of an arbitrary elastic shell-type structure of revolution subjected to arbitrary applied dynamical loadings and an external pressure. In this model, the structure is composed of a finite number of shells of revolution, each in the shape of a conical frustum, so the the model can be used to study an arbirary shell of revolution to which is attached arbitrarily shaped circumferential ring stiffeners and lateral bulkheads. This model and the computer program based on the model is intended to be used as an analysis subprogram in an automated structural design algorithm.

Computer programs for the analysis of complex assemblies of shells of revolution have been in existence for nearly a decade [1,2], and in particular the BOSOR computer code [2], has received wide spread acceptance and usage in the engineering community. Codes of this type are necessarily developed for user ease and convenience, with special features designed (a) to ease preparation and checking of computer models of the structure and (b) to provide comprehensive data manipulation and display features to assist the user in interpreting results. Unfortunately, these features make the codes very difficult to employ in the development of an automated structural synthesis program. In such a program, the analysis of a shell of revolution is a subprogram (or subroutine) which must be called and exercised many times during the course of the automated structural design procedure. Thus the analysis subprogram must be as efficient as possible and be written to minimize computer storage requirements, with no user convenience packages.

The difficulties in developing such an analysis subprogram are evident, since to date design optimization algorithms [3,4,5] have been capable of dealing only with simple structural configurations such as cylindrical shells stiffened by only simple T-ring stiffeners. Analyses have been based upon equivalent orthotropic shell models, which are unable to account for the effects of discrete stiffeners.

The finite element model for the conical frustum presented in this report is based on Flugge-Lure-Byrne third order shell theory [6], in which a coupling exists in the shell constitutive relations between bending and membrane effects. Stiffness and kinetic energy functionals are used to derive "consistent" stiffness and mass matrices. Bolotin's functional for initial stress [7] and Cohen's representation for the potential due to external pressure [8] are used to generate the so called "geometric stiffness" matrices required for the study of the effects of external pressure on structural stability. All variables in the system are represented by means of a Fourier series in the circumferential angle θ. Except for the stability functional a complete decoupling exists between variables with differing circumferential mode numbers so that only variables associated with a given circumferential mode number n interact. In order to decompose the stability functional the initial stress state of the structure is assumed to be symmetric, i.e., only the initial stresses associated with n=0 are considered, with both membrane and bending stress resultants taken into account.

The kinematical behavior of each Fourier component of the displacement field of the conical frustum is defined by a polynomial function of position along the shell generator. Two

different models are defined based on the complexity of this assumed displacement field. For the first, simpler model, the normal (outward) displacement is represented by a third order polynomial and the in surface displacements are of first order. Therefore, this model is similar to that in [1] although the element in [1] is based on a Donnell-Mushtari-Vlasov theory. This model results in a nodal ring at each end of the conical frustum around which three nodal displacements and one rotation are defined. Thus, this element has eight nodal displacement degrees-of-freedom.

The second, more complex, element utilizes a fifth order polynomial representation for the normal displacement and second order polynomials for the surface displacements, resulting in a model with three nodal rings and twelve nodal displacement degrees-of-freedom.

Integration of the energy forms required for determination of the coefficients of the stiffness, mass and stability matrices is accomplished by use of Gaussian quadrature formulas, using three through ten point interpolation formulas.

Section II describes the general analytical development of the finite element model and Section III gives the matrix forms which describe the stiffness, mass and stability (initial stress) characteristics for the element. Section IV is a brief description of the computer code required to generate the element properties and of some of the sample problems run to date.

II. ANALYTICAL DEVELOPMENT

II.1 Model of Conical Frustum.

In order to model a complex shell of revolution, it is first necessary to develop an analytical representation for a frustum of a conical shell, see Figure 1. For this frustum let ϕ denote the angle between the (straight) shell generator and its axis of symmetry, s denote the distance along the generator, (assumed to be the middle surface of the shell). Then $-s_o<s<s_o$, where $2s_o$ is the length of the generator of the shell. Also, let θ denote the circumferential angle and $\frac{r_1+r_2}{2} + \frac{r_2-r_1}{2} \cdot \frac{s}{s_o} = r$ be the distance from the generator at s to the axis of the shell, where r_1 and r_2 are the radii of the circles at $s = -s_o$ and $s = s_o$, respectively. For a conical shell, the principal radii of curvature for the middle surface of the shell are $R_1 = r \sec \phi$ and $R_2 = \infty$ in the circumferential and meridional direction, respectively. Finally, let ζ be the ordinate perpendicular to the shell surface as shown in Figure 1 and let t denote time. Then, assuming that the shell obeys Love's postulate [6] the complete behavior of the shell is described in terms of middle surface displacements $u(\theta,s,t)$, $v(\theta,s,t)$ and $w(\theta,s,t)$ acting in the meridional, circumferential and normal directions to the shell surface (positive outward), respectively. That is, all points in the shell move according to the relations [6] .

$$u_\theta = v\left(1 + \frac{\zeta}{r}\cos\phi\right) - \frac{\zeta}{r} w_{,\theta} \qquad (1a)$$

$$u_s = u - \zeta w_{,s} \qquad (1b)$$

$$u_\zeta = w \qquad (1c)$$

where u_θ, u_s, and u_ζ are motions of a point at s, θ, ζ in the circumferential, meridional and normal directions, respectively.

In order to develop expressions for the internal energies associated with initial and elastic effects, gradients of the displacement field are required, written in orthogonal curvilinear conical shell coordinates. The components associated with gradient of the ith displacement in the jth direction, written $\nabla_{i\,j} u$, are as follows [9], written as a 3 x 3 matrix.

$$\begin{bmatrix} \nabla_{1\,1} u & \nabla_{1\,2} u & \nabla_{1\,3} u \\ \nabla_{2\,1} u & \nabla_{2\,2} u & \nabla_{2\,3} u \\ \nabla_{3\,1} u & \nabla_{3\,2} u & \nabla_{3\,3} u \end{bmatrix} = \begin{bmatrix} \frac{1}{R}\left(u_{\theta,\theta} + u_s \sin\phi + u_\zeta \cos\phi\right) & \frac{1}{R}\left(u_{s,\theta} - u_s \sin\phi\right) & \frac{1}{R}\left(u_{\zeta,\theta} - u_\theta \cos\phi\right) \\ u_{\theta,s} & u_{s,s} & u_{\zeta,s} \\ u_{\theta,\zeta} & u_{s,\zeta} & u_{\zeta,\zeta} \end{bmatrix} \tag{2}$$

where $R = r + \zeta \cos\phi$.

Note that the components of the symmetric portion of this matrix are the local strain components ϵ_{ij},

$$\begin{bmatrix} \epsilon_{11} & \epsilon_{12} & \epsilon_{13} \\ \epsilon_{21} & \epsilon_{22} & \epsilon_{23} \\ \epsilon_{31} & \epsilon_{32} & \epsilon_{33} \end{bmatrix} =$$

$$\begin{bmatrix} \frac{1}{R}\left(u_{\theta,\theta} + u_s \sin\phi + u_\zeta \cos\phi\right) & \frac{1}{2}\left(u_{\theta,s} + \frac{1}{R} u_{s,\theta} - \frac{u_s}{R} \sin\phi\right) & \frac{1}{2}\left(u_{\theta,\zeta} + \frac{1}{R} u_{\zeta,\theta} - \frac{u_\theta}{R} \cos\phi\right) \\ & u_{s,s} & \frac{1}{2}\left(u_{s,\zeta} + u_{\zeta,s}\right) \\ \text{symmetric} & & u_{\zeta,\zeta} \end{bmatrix} \tag{3}$$

The strains associated with row 3 and column 3 are zero as a consequence of Eq. (1).

II.2 Strain Energy of Shell

The strain energy per unit surface area U_o of a thin isotropic elastic shell is given by the integral

$$U_o = \frac{1}{2}\frac{E}{(1-\nu^2)}\int_{-\frac{h}{2}}^{\frac{h}{2}}\left[\epsilon_{\theta s}^2 + 2\nu\epsilon_{\theta\theta}\epsilon_{ss} + \epsilon_{ss}^2 + 2(1-\nu)\epsilon_{\theta s}^2\right]\cdot \tag{4}$$

$$\cdot\left(1+\frac{\zeta}{r}\cos\phi\right)d\zeta$$

where E is Young's Modulus, ν is Poisson's ratio and h is the shell thickness.

Substitution of Eq. (3) into (4), with the aid of Eq. (1), gives, according to the 3rd order Flügge-Luré-Byrne theory [6].

$$U_o = \frac{1}{2}\left[N_\theta\epsilon_\theta + N_s\epsilon_s + \left(N_{\theta s} + N_{s\theta} - \frac{M_{\theta s}}{R_1}\right)\epsilon_{\theta s}\right. \tag{5}$$

$$\left. + M_\theta\kappa_\theta + M_s\kappa_s + \left(M_{\theta s} + M_{s\theta}\right)\kappa_{s\theta}\right]$$

where

$$\epsilon_\theta = \frac{1}{r}(u_{,\theta} + u\sin\phi + w\cos\phi)$$

$$\epsilon_s = u_{,s} \tag{6}$$

$$\epsilon_{\theta s} = \epsilon_{s\theta} = \frac{1}{2}\left(\frac{1}{r}u_{,\theta} + v_{,s} - \sin\phi\cdot v\right)$$

are the shell surface (membrane) strains, and

$$\kappa_\theta = \left[\frac{1}{r}\frac{\cos\phi}{r}v_{,\theta} - \frac{1}{r}w_{,\theta\theta} - \sin\phi\, w_{,s}\right]$$

$$\kappa_s = -w_{,ss} \tag{7}$$

$$\kappa_{\theta s} = \kappa_{s\theta} = \frac{\cos\phi}{r}\left(v_{,s} - \frac{\sin\phi}{r}v\right) + \frac{1}{r}\left(\frac{\sin\phi}{r}w_{,\theta} - w_{,s\theta}\right)$$

are changes in the surface curvature of the shell. The symbols N_{ij} and M_{ij} $i,j=\theta,s$ are the shell membrane stress resultants and shell bending moments, respectively, and are related to the strain measures, ϵ_y and κ_y according to the relations

$$N_\theta = C\left(\epsilon_\theta + \nu\epsilon_s\right) + D\left(\frac{\cos\phi}{r}\right)\left(\epsilon_\theta\frac{\cos\phi}{r} - \kappa_\theta\right)$$

$$N_s = C\left(\epsilon_s + \nu\epsilon_\theta\right) + D\left(\frac{\cos\phi}{r}\right)\kappa_s \qquad (8a)$$

$$N_{\theta s} = C(1-\nu)\cdot\epsilon_{\theta s} + D(1-\nu)\frac{\cos\phi}{r}\left(\frac{\cos\phi}{r}\epsilon_{\theta s} - \frac{\kappa_{\theta s}}{2}\right)$$

$$N_{s\theta} = C(1-\nu)\cdot\epsilon_{s\theta} + D(1-\nu)\frac{\cos\phi}{r}\cdot\frac{\kappa_{\theta s}}{2}$$

$$M_\theta = D\left(\kappa_\theta + \nu\kappa_s - \epsilon_\theta\frac{\cos\phi}{r}\right)$$

$$M_s = D\left(\kappa_s + \nu\kappa_\theta + \epsilon_s\frac{\cos\phi}{r}\right) \qquad (8b)$$

$$M_{\theta s} = D(1-\nu)\left(\kappa_{\theta s} - \epsilon_{\theta s}\frac{\cos\phi}{r}\right)$$

$$M_{s\theta} = D(1-\nu)\,\kappa_{s\theta}$$

where $C = Eh/(1-\nu^2)$ and $D = Eh^3/\left(12(1-\nu^2)\right)$

Note that

$$N_{\theta s} + \frac{M_{\theta s}}{R_1} \equiv N_{s\theta} \qquad (9)$$

II.3 Kinetic Energy

The kinetic energy of the shell per unit surface area is given by the integral

$$T_o = \frac{\rho}{2}\int_{-h/2}^{h/2} (\dot{u}_\theta^2 + \dot{u}_s^2 + \dot{u}_\zeta^2)(1 + \frac{\zeta\cos\phi}{r})d\zeta \tag{10}$$

In (10) the dot denotes differentiation with respect of time t. Since u_θ, u_s and u_ζ are related to the surface displacements v,u and w according to Eqs. (1), substitution of Eqs. (1) into Eq. (10) gives

$$T_o = \frac{\rho h}{2}\left\{\left(1 + \frac{h^2\cos^2\phi}{4r^2}\right)\dot{v}^2 + \dot{u}^2 + \dot{w}^2 - \frac{h^2\cos\phi}{6r^2}\cdot\left(2\dot{v}\dot{w}_{,\theta} + r\dot{u}\dot{w}_{,s}\right) + \frac{h^2}{12}\left(\frac{1}{r^2}\dot{w}_{,\theta}^2 + \dot{w}_{,s}^2\right)\right\} \tag{11}$$

II.4 Potential for Initial Stress

As indicated by Bolotin [7], the potential per unit surface area U_{go} associated with small shell motions v,u,w away from an initial equilibrium state with stresses σ_{jk} is given by the quadratic form

$$U_{go} = \frac{1}{2}\int_{-\frac{h}{2}}^{h/2} \sigma_{jk}\left(\nabla_j u_i\right)\left(\nabla_k u_i\right)dz \tag{12}$$

where the $\nabla_j u_i$ are the displacement gradients in Eqs. (2), and summation is implied on the subscripts i,j,k. After substitution of Eqs. (1) into (2) and recognizing that Love's postulate requires $\sigma_{sz} = \sigma_{\theta z} = \sigma_{zz} = 0$, integration through the shell thickness gives

$$
\begin{aligned}
U_{go} = \frac{1}{2}\Bigg\{ & \frac{N^{o}_{\theta}}{r}\Big\{ v^2 + v_{,\theta}^2 + (\sin\phi\, u + \cos\phi\, w)^2 + u_{,\theta}^2 + w_{,\theta}^2 \\
& + 2v_{,\theta}(\sin\phi\, u + \cos\phi\, w) - 2v(\sin\phi\, u_{,\theta} + \cos\phi\, w_{,\theta}) \Big\} + \\
& + M^{o}_{\theta}\frac{\cos\phi}{r}\Big\{ v^2 + v_{,\theta}^2 - u_{,\theta}^2 + w_{,\theta}^2 - (\sin\phi\, u + \cos\phi\, w)^2 \\
& - 2w(w_{,\theta\theta} + r\sin\phi\, w_{,s}) - \frac{2}{\cos\phi}\Big[(v_{,\theta} + \sin\phi\, u)(w_{,\theta\theta} + r\sin\phi\, w_{,s}) \\
& + u_{,\theta}(w_{,s\theta}\, r - \sin\phi\, w_{,\theta}) + v(r\sin\phi\, w_{,s\theta} - w_{,\theta}) \Big] \Big\} \\
& + N^{o}_{s}\Big\{ v_{,s}^2 + u_{,s}^2 + w_{,s}^2 \Big\} + \frac{M^{o}_{s}}{r}\Big\{ 2v_{,s}\Big[\cos\phi\, v_{,s} - w_{,\theta s} \\
& - \frac{\sin\phi}{r}(\cos\phi\, v - w_{,\theta}) \Big] - 2r w_{,ss}\, u_{,s} \Big\} \\
& + \frac{N^{o}_{s\theta}}{r}\Big\{ 2v_{,s}(\sin\phi u + \cos\phi w) - 2v(\sin\phi\, u_{,s} + \cos\phi\, w_{,s}) \\
& + 2v_{,s}\, v_{,\theta} + 2w_{,s}\, w_{,\theta} + u_{,s}\, u_{,\theta} \Big\} + \frac{N^{o}_{\theta s}}{r}\Big\{ u_{,s}\, u_{,\theta} \Big\} \\
& + \left(M^{o}_{s\theta} + \frac{M^{o}_{\theta s}}{r} \right)\Big\{ (v_{,\theta} + \sin\phi\, u + \cos\phi\, w)\left(-w_{,\theta s} + \frac{\sin\phi}{r}(w_{,\theta} - \cos\phi\, v) \right) \\
& + v_{,s}(\cos\phi\, v_{,\theta} - w_{,\theta\theta} - r\sin\phi\, w_{,s}) \\
& + r\, w_{,ss}(\sin\phi\, v - u_{,\theta}) - u_{,s}(r w_{,s\theta} + \sin\phi\, w_{,\theta}) \Big\} \\
& - \frac{1}{2r} M^{o}_{s\theta}\Big\{ u_{,s}\, u_{,\theta}\cos\phi \Big\}
\end{aligned}
\tag{13}
$$

Note that in Eq. (13) all N_{ij} and M_{ij} have superscripts (^{o}) which denotes the initial stresses. In utilizing this expression

$$N^o_{ij} \equiv \beta N^e_{ij}, \quad M^o_{ij} \equiv \beta M^e_y \tag{14}$$

where N^e_{ij}, M^e_{ij} denote the stress resultants obtained from an analysis in which initial stress effects are ignored and β is a scale factor.

II.5 External Potential Due to Pressure Loadings.

As discussed by Cohen [8] normal pressure loadings, which are follower type forces, will admit to a quadratic potential only for certain special conditions on the boundaries of the shell. For this restricted case, the external potential per unit undeformed surface is a functional given by the expression

$$U_{eo} = \beta \cdot \frac{p^e}{r} \left[(v, _\theta + \sin\phi \; u + ru, _s) \cdot w + \frac{1}{2} \cos\phi (v^2 + w^2) \right] \tag{15}$$

The pressure p^e is the loading which is used to generate the N^e_{ij} and M^e_{ij} in Section II.4, and, as shown in Figure 1, is assumed to act in a direction opposite to that of w. In this form p^e is assumed to be independent of s, θ.

II.6 Hamiltonian for Shell.

The Hamiltonian used to characterize the behavior of the conical frustum of the shell is the integral of the potentials in Sections II.3-5 over the surface of the shell,

$$H = T - V = \int_0^{2\pi} \int_{-s_o}^{s_o} \left[T_o - (U_o + U_{go} + U_{eo} + V_e) \right] r \, d\theta \, ds \tag{16}$$

This functional gives all the information required to model the shell. Although a set of differential equations and associated boundary conditions could be derived, in order to develop an algebraic representation of the structure, a Fourier series is used to specify the dependence of the shell variables in the circumferential angle θ, and an explicit polynomial representation is used to specify the dependence in s.

II.7 Fourier Analysis.

Since the shell is closed, i.e., $0 \leqslant \theta \leqslant 2\pi$ all variables required to describe the shell may be expanded into a Fourier series in the circumferential angle θ. In particular

$$
\begin{aligned}
v(s,\theta) &= v^{*o}(s) - \sum_{n=1}^{N} v^{n}(s)\sin n\theta + \sum_{n=1}^{N} v^{*n}\cos n\theta \\
u(s,\theta) &= u^{o}(s) + \sum_{n=1}^{N} u^{n}(s)\cos n\theta + \sum_{n=1}^{N} u^{*n}\sin n\theta \qquad (17) \\
w(s,\theta) &= w^{o}(s) + \sum_{n=1}^{N} w^{n}(s)\cos n\theta + \sum_{n=1}^{N} w^{*n}\sin n\theta
\end{aligned}
$$

where n is the circumferential mode number and N is the maximum number of Fourier forms considered in the analysis. Substitution of Eqs. (17) into Eqs. (16) and integration will remove the angle θ from the functional, at the expense of introducing the scalar parameter n=1,---,N. Fortunately, the portions of the Hamiltonian associated with U_o and T_o are quadratic in all the field variables so that, due to the orthogonality of the Fourier series, a complete decoupling occurs between variable sets with differing mode number n. Further, all variables with asterisk (*) decouple with the variable not so labeled, so that a major simplification exists

in using a Fourier series so far as U_o and T_o are concerned.

Unfortunately, the simplifying features associated with the quadratic forms for U_o and T_o do not carry over to the more complex potentials associated with initial stresses, and external pressure, since in these potentials three field variables interact, two displacement gradients and an initial stress. Thus axisymmetric initial stresses interact with sets of functions for all mode numbers and non-axisymmetric initial stresses will couple all the harmonics together.

In order to attempt to develop a useful analysis and obtain a tractable computer program only the initial stresses associated with n=0 and symmetric (v=0) motion are considered. That is, only the initial effects associated with p_e^o, N_θ^o, N_s^o, M_θ^o and M_s^o are included in the geometric and (quadratic) external potentials. Torsional prestresses $N_{s\theta}^e$, $M_{s\theta_n}^e$ and $M_{s\theta_n}^e$ will, for a given wave number n, couple the motions u_i^n with u_i^{n*} and so will not be considered at this time.

Given the special form of the initial stress and external potential described in Section II.6, then a complete decoupling of the shell energies is possible and the analysis of the shell may be carried out one mode at a time. For each mode the potentials may be written as matrix forms

$$U_n = \frac{\pi}{2}\int_L \left(\left|\delta_n\right|^T \left[\tilde{K}_n\right] \left|\delta_n\right| + \left|\delta_n^*\right|^T \left[\tilde{K}_n\right] \left|\delta_n^*\right| \right) rds \tag{18a}$$

$$T_n = \frac{\pi}{2}\int_L \left(\left|\dot{\delta}_n\right|^T \left[\tilde{M}_n\right] \left|\dot{\delta}_n\right| + \left|\dot{\delta}_n^*\right|^T \left[\tilde{M}_n\right] \left|\dot{\delta}_n^*\right| \right) rds \tag{18b}$$

$$U_{gn} + U_{en} = \frac{\beta\pi}{2}\int_L \left(\left|\delta_n\right|^T \left[\tilde{G}_n^s\right] \left|\delta_n\right| + \left|\delta_n^*\right|^T \left[\tilde{G}_n^s\right] \left|\delta_n^*\right| \right) rds \tag{18c}$$

where

$$\left|\delta_n\right|^T = \left\langle u_n \quad u_{n,s} \quad w_n \quad w_{n,s} \quad w_{n,ss} \quad v_n \quad v_{n,s} \right\rangle \tag{19}$$

and $\left|\delta^*_n\right|$ is identical to $\left|\delta_n\right|$ except that an asterisk appears on all the vector components.

The matrices $\left[\widetilde{K}_n\right]$, $\left[\widetilde{M}_n\right]$ and $\left[\widetilde{G}_n\right]$ are shown in Figures 2,3 and 4, respectively. Since the quadratic forms in $\left|\delta^*_n\right|$ and $\left|\dot{\delta}^*_n\right|$ are identical to the ones for $\left|\delta_n\right|$ and $\left|\dot{\delta}_n\right|$ it is necessary to directly deal only with $\left|\delta_n\right|$ and $\left|\dot{\delta}_n\right|$.

III. SHELL FINITE ELEMENT

III.1 Approximation of Displacement Field.

Except for the simplifications used in the initial stress and external potentials, the energy forms in Eqs. (18) are exact to order h^3, and may be used to develop differential equations in the variables $v^n(s,t)$, $u^n(s,t)$ and $w^n(s,t)$. However, a much simpler, and yet accurate representation of the behavior of the frustum can be achieved by representing the displacements as polynomial functions of the meridional position $s' = s/s_o$. In this report two different polynomial representations are used. For the first (Type I representation)

$$
\begin{aligned}
u^n(s,t) &= \alpha_{u1}^n + \alpha_{u2}^n s' \\
w^n(s,t) &= \alpha_{w1}^n + \alpha_{w2}^n s' + \alpha_{w3}^n s'^2 + \alpha_{w4}^n s'^3 \qquad \text{(20a)} \\
v^n(s,t) &= \alpha_{v1}^n + \alpha_{v2}^n s'
\end{aligned}
$$

where the α's are time dependent functions.

For the second, Type II element

$$
\begin{aligned}
u^n(s,t) &= \alpha_{u1}^n + \alpha_{u2}^n s' + \alpha_{u3}^n s'^2 \\
w^n(s,t) &= \alpha_{w1}^n + \alpha_{w2}^n s' + \alpha_{w3}^n s'^2 + \alpha_{w4}^n s'^3 + \alpha_{w5}^n s'^4 + \alpha_{w6}^n s'^5 \qquad \text{(20b)} \\
v^n(s,t) &= \alpha_{v1}^n + \alpha_{v2}^n s' + \alpha_{v3}^n s'^2
\end{aligned}
$$

Thus the shell surface displacements and displacement derivatives $\left|\delta_n\right|$ may be expressed through the meridionally dependent transformation $\Delta(s')$ in terms of the polynomial coefficients $\left|\alpha_n\right|$, defined for the frustum as a whole

$$\left|\delta_n^I(s',t)\right| = \left[\Delta(s')^I\right] \left|\alpha_n^I(t)\right| \tag{21}$$

A similar expression holds for the Type II element. The time dependent constants may in turn be defined in terms of shell displacements at specified positions along the meridion using Hermite's Formula [9]. For the Type I element the locations chosen are $s = -s_o$ and $s = +s_o$. At each location i four quantities are defined, u_i^n, v_i^n, w_i^n and $w_{i,s}^h$. These shell displacements may in turn be transformed into displacements $\bar{u}_i^n$, $\bar{v}_i^n$, $\bar{w}_i^n$ and $\bar{\beta}_i^n$, termed <u>nodal</u> displacements (Fig. 5) which are shell displacements in the axial, circumferential, radial (not normal) directions and rotation, such that

$$\begin{aligned}
u_i^n &= \bar{u}_i^n \cos\phi + \bar{w}_i^n \sin\phi \\
v_i^n &= \bar{v}_i^n \\
w_i^n &= -\bar{u}_i^n \sin\phi + \bar{w}_i^n \cos\phi \\
w_{i,s}^n &= \bar{\beta}_i^n
\end{aligned} \tag{22}$$

The results, in matrix form are as follows for the Type I element. In this matrix C is $\cos\phi$ and S is $\sin\phi$.

$$
\begin{Bmatrix} \alpha^{n}_{u1} \\ \alpha^{n}_{u2} \\ \alpha^{n}_{w1} \\ \alpha^{n}_{w2} \\ \alpha^{n}_{w3} \\ \alpha^{n}_{w4} \\ \alpha^{n}_{v1} \\ \alpha^{n}_{v2} \end{Bmatrix} =
\left[\begin{array}{cccc|cccc}
C/2 & S/2 & 0 & 0 & C/2 & C/2 & 0 & 0 \\
-C/2 & -S/2 & 0 & 0 & C/2 & S/2 & 0 & 0 \\
-S/2 & C/2 & s_o/4 & 0 & -S/2 & C/2 & -s_o/4 & 0 \\
3S/4 & -3C/4 & -s_o/4 & 0 & -3S/4 & 3C/4 & -s_o/4 & 0 \\
0 & 0 & -s_o/4 & 0 & 0 & 0 & -s_o/4 & 0 \\
-S/4 & C/4 & s_o/4 & 0 & S/4 & -S/4 & -s_o/4 & 0 \\
0 & 0 & 0 & 1/2 & 0 & 0 & 0 & 1/2 \\
0 & 0 & 0 & -1/2 & 0 & 0 & 0 & 1/2
\end{array}\right]
\begin{Bmatrix} \bar{u}^{n}_{i} \\ \bar{w}^{n}_{i} \\ \bar{\beta}^{n}_{i} \\ \bar{v}^{n}_{i} \\ \bar{u}^{n}_{j} \\ \bar{w}^{n}_{j} \\ \bar{\beta}^{n}_{j} \\ \bar{v}^{n}_{j} \end{Bmatrix} \qquad (23)
$$

or,

$$
\begin{Bmatrix} \alpha^{I}_{n} \end{Bmatrix} = \begin{bmatrix} I \\ A\,(\phi, s_o) \end{bmatrix} \begin{Bmatrix} q^{I}_{n} \end{Bmatrix} \qquad (24)
$$

In Eqs. (23,24) node i is at $s = -s_o$ and node j is at $s = +s_o$. For Type II elements the relation is similar,

$$
\begin{Bmatrix} \alpha^{n}_{u1} \\ \alpha^{n}_{u2} \\ \alpha^{n}_{u3} \\ \alpha^{n}_{w1} \\ \alpha^{n}_{w2} \\ \alpha^{n}_{w3} \\ \alpha^{n}_{w4} \\ \alpha^{n}_{w5} \\ \alpha^{n}_{w6} \\ \alpha^{n}_{v1} \\ \alpha^{n}_{v2} \\ \alpha^{n}_{v3} \end{Bmatrix} =
\left[\begin{array}{cccc|cc|cc|cc|cc}
0 & 0 & 0 & 0 & C & S & 0 & 0 & 0 & 0 & 0 & 0 \\
-C/2 & -S/2 & 0 & 0 & 0 & 0 & 0 & 0 & C/2 & S/2 & 0 & 0 \\
C/2 & S/2 & 0 & 0 & -C & -S & 0 & 0 & C/2 & S/2 & 0 & 0 \\
0 & 0 & 0 & 0 & -S & C & 0 & 0 & 0 & 0 & 0 & 0 \\
0 & 0 & 0 & 0 & 0 & 0 & s_o & 0 & 0 & 0 & 0 & 0 \\
-S/2 & C & s_o/4 & 0 & 2S & -2C & 0 & 0 & -S & C & -s_o/4 & 0 \\
5S/4 & -5C/4 & -s_o/4 & 0 & 0 & 0 & -2s_o & 0 & -5S/4 & 5C/4 & -s_o/4 & 0 \\
S/2 & -C/2 & -s_o/4 & 0 & -S & C & 0 & 0 & S/2 & -C/2 & s_o/4 & 0 \\
-3S/4 & 3C/4 & s_o/4 & 0 & 0 & 0 & s_o & 0 & 3S/4 & -3C/4 & s_o/4 & 0 \\
0 & 0 & 0 & 0 & 0 & 0 & 0 & 1 & 0 & 0 & 0 & 0 \\
0 & 0 & 0 & -1/2 & 0 & 0 & 0 & 0 & 0 & 0 & 0 & 1/2 \\
0 & 0 & 0 & 1/2 & 0 & 0 & 0 & -1 & 0 & 0 & 0 & 1/2
\end{array}\right]
\begin{Bmatrix} \bar{u}^{n}_{i} \\ \bar{w}^{n}_{i} \\ \bar{\beta}^{n}_{i} \\ \bar{v}^{n}_{i} \\ \bar{u}^{n}_{j} \\ \bar{w}^{n}_{j} \\ \bar{\beta}^{n}_{j} \\ \bar{v}^{n}_{j} \\ \bar{u}^{n}_{k} \\ \bar{w}^{n}_{k} \\ \bar{\beta}^{n}_{k} \\ \bar{v}^{n}_{k} \end{Bmatrix} \quad (25
$$

or

$$
\begin{Bmatrix} \alpha^{I}_{n} \end{Bmatrix} = \begin{bmatrix} A^{II}_{o}(\phi, s) \end{bmatrix} \begin{Bmatrix} q^{II}_{n} \end{Bmatrix} \qquad (26)
$$

In Eqs. (25,26) nodes i,j,k are at $s = -s_o, 0$, and s_o respectively.

The finite element model is then described by the following energy forms, for the Type I element:

$$
\begin{aligned}
U_n^I &= \frac{\pi s_o}{2}\left\{q_n^I\right\}^T\left[A^I\right]^T\pi\int_{-1}^{1}\left[\Delta^I\right]^T\left[\tilde{K}_n\right]\left[\Delta^I\right]rds'\cdot\left[A^I\right]\left\{q_n^I\right\} \\
T_n^I &= \frac{\pi s_o}{2}\left\{\dot{q}_n^I\right\}^T\left[A^I\right]^T\int_{-1}^{1}\left[\Delta^I\right]^T\left[\tilde{M}_n\right]\left[\Delta^I\right]rds'\cdot\left[A^I\right]\left\{\dot{q}_n^I\right\} \qquad (27) \\
U_{gn}^I + U_{en}^I &= \frac{\pi s_o}{2}\left\{q_n\right\}^T\left[A^I\right]^T\int_{-1}^{1}\left[\Delta^I\right]^T\left[\tilde{G}_n\right]\left[\Delta^I\right]rds'\cdot\left[A^I\right]\left\{q_n^I\right\}
\end{aligned}
$$

Energy expressions for the Type II element are identical except that superscript II appears in place of I. Equations (27) may be simplified to read

$$
\begin{aligned}
U_n^I &= \frac{1}{2}\left\{q_n^I\right\}^T\left[K_n^I\right]\left\{q_n^I\right\} \\
T_n^I &= \frac{1}{2}\left\{\dot{q}_n^I\right\}^T\left[M_n^I\right]\left\{\dot{q}_n^I\right\} \qquad (28) \\
U_{gn}^I + U_{en}^I &= \frac{\beta}{2}\left\{q_n^I\right\}^T\left[G_n^I\right]\left\{q_n^I\right\}
\end{aligned}
$$

Similarly, expressions hold for Type II elements in Eqs. (28) matrices $\left[K_n^I\right]$, $\left[M_n^I\right]$ and $\left[G_n^I\right]$ are the stiffness, mass and geometric stiffness for the shell element. Application of Hamilton's principle gives the equations which characterize the vibration and stability characteristics of the frustum using the Type I element,

$$\left[{}^{I}_{M_n}\right]\left\{{}^{I}_{\ddot{q}_n}\right\} + \left(\left[{}^{I}_{K_n}\right] + \beta\left[{}^{I}_{G_n}\right]\right)\left\{{}^{I}_{q_n}\right\} = \left\{0\right\} \tag{29}$$

This equation has eight independent degrees of freedom. Equations similar to Eqs. (29) hold for the Type II element, but have twelve degrees of freedom.

III.2 Numerical Aspects of Finite Element.

The matrices characterizing stiffness mass and shell stability of the type in Eqs. (27) are very complex functions of the ordinate s. Therefore, these matrices are evaluated numerically using Gaussian quadrature formulas, with variable point integrations depending upon the degree of accuracy required. In detail, the matrix expressions in Eq. (27), e.g., $\left[{}^{I}_{\Delta}\right]^{T}\left[{}^{I}_{K_n}\right]\left[{}^{I}_{\Delta}\right]$ are first multiplied and evaluated at the required Gaussian points, weighting factors are then multiplied to the matrix, and the result is stored. Results are accumulated in storage as the program progresses through the various integration points. It should be noted that since the element matrices are symmetric only diagonal and upper triangular portion need be calculated, and also that a formal matrix product may be replaced with much simpler and more efficient direct statements of the matrix product.

III.3 External Potential

In order to implement the conical frustam element in the solution of a finite element forced response problem it is necessary to develop the linear external potential of the applied loads. These loads are either statical or dynamical and are distributed upon the surface of the elements and around the nodal rings of

the assemblage of elements. A stability problem is not a linear forced response problem, but in order to calculate the prestress state it is first necessary to perform a static analysis.

Two sets of applied loads are defined. The first set is the surface loads f_s, f_θ and f_ζ, assumed to be applied to the middle surface of the shell, permit undeformed surface area, in the s, θ and ζ directions, respectively, see Figure 5. (The contribution to the external potential due to the pressure acting on the deformed surface area is accounted for in Eq. (15).)

These surface loads are functions of s and θ and may be represented by the Fourier series

$$f_s(s,\theta) = f_s^o(s) + \sum_{n=1}^{N}\left[f_s^n(s)\cos n\theta + f_s^{*n}\sin n\theta\right]$$

$$f_\zeta(s,\theta) = \left[f_\zeta^o(s)-p(s)\right] + \sum_{n=1}^{N}\left[f_\zeta^n(s)\cos n\theta + f_\zeta^{*n}\sin n\theta\right] \qquad (30)$$

$$f_\theta(s,\theta) = f_\theta^{*o}(s) + \sum_{n=1}^{N}\left[-f_\theta^n(s)\sin n\theta + f_\theta^{*n}\cos n\theta\right]$$

The second set of applied loads are line loads F_z, F_r, M_β and F_θ are simply forces and a moment per unit circumferential length which are applied around the nodal rings and are represented in terms of a Fourier series (F_z, F_r and M_β are similar)

$$F_z(\theta) = F_{z_o}^o + \sum_{n=1}^{N}\left(F_z^n\cos n\theta + F_z^{*n}\sin n\theta\right)$$

$$F_r(\theta) = F_r^o + \sum_{n=1}^{N}\left(F_r^n\cos n\theta + F_r^{*n}\sin n\theta\right)$$

$$F_\theta(\theta) = F_\theta^{*o} + \sum_{n=1}^{N}\left(-F_\theta^n\sin n\theta + F_\theta^{*n}\cos n\theta\right)$$

Eq. (31) continued

$$M_\beta(\theta) = M_\beta^o + \sum_{n=1}^{N} \left(M_\beta^n \cos n\theta + M_\beta^{*n} \sin n\theta\right) \tag{31}$$

The external potential of the ring loads at node i denoted V_{e_i} is then

$$V_{e_i} = -\int_o^{2\pi} \left(F_{z_i}(\theta)\bar{u}_i(\theta) + F_{r_i}\bar{w}_i + M_{\beta_i} + F_{\theta_i}\bar{v}_i\right)r \, d\theta \tag{32}$$

Due to the orthogonality of the functions in θ the forces decouple into harmonics in wave number n and similar expressions for the n^{*} series at node i. The equivalent nodal load for the n^{th} harmonic, $\{F_i^n\}$, is thus given as

$$V_{e_i}^n = -\pi r_i \left[F_z^n \bar{u}^n + F_r^n \bar{w}^m + M_\beta^n \bar{\beta}^n + F_\theta^n \bar{v}^n\right]_i \tag{33}$$

The external potential of the surface loads on element m is written as V_{e_m} is expressed by the integral

$$V_{e_m} = -\int_o^{2\pi} \int_{-s_o}^{s_o} \left[f_s(s,\theta)u(s,\theta) + f_\zeta w + f_\theta v\right]r(s)\,ds\,d\theta \tag{34}$$

Expressing the surface loads as the vector $\{f\}^T = \{f_s\ f_\zeta\ f_\theta\}$ and using the element transformations defined previously the surface loads may be converted into equivalent nodal loads $\{F_m^n\}$ acting on the nodes connected to element m, $\{q_m^n\}$, as

$$V_{e_m}^n = -\pi s_o \{q_m^n\}^T \left[A\right]^T \int_{-1}^{1} \left[\Delta(s')\right]^T \{f^n(s')\} r(s')\,ds' \tag{35}$$

$$= -\{q_m^n\}^T \{F_m^n\}$$

As implemented in the computer program at present the integration in s' to compute surface loads is carried out in closed form for surface loads assumed to be constant over each element.

III.4 Assemblage of Global Model

Using the conical frustum element it is possible to model any shell of revolution to any degree of accuracy required using a sufficient number of elements. Shells having meridional curvature such as spherical shells will require relatively more elements since the element itself lacks meridional curvature. However shells composed of cylindrical, conical and circular disk components may be modelled with very few elements, especially when using the higher order Type II element. Assuming the global model to have I nodes then the system will have four degrees of freedom per node ($\bar{u}_i^n$, $\bar{w}_i^n$, $\bar{\beta}_i^n$ and $\bar{v}_i^n$) or 4I degrees of freedom. The system degrees of freedom are assembled in the vector $\{\bar{q}^n\}$. System stiffness, geometric stiffness and mass matrices $\left[K^n\right]$, $\left[G^n\right]$ and $\left[M^n\right]$ are formed by adding up the element matrices taking into account the nodal connectivities of the individual elements. Similarly, the system force vector $\{\bar{F}^n\}$ is formed by adding up all the equivalent nodal loads due to ring loads and elemental surface loads. If the elements are assembled sequentially and there are no branches or closed loops in the structure. The resultant equations will be highly banded. Using only Type I elements the bandwidth will be only 8 degrees of freedom and using Type II elements will result in a bandwidth of 12.

Assuming a time dependence for dynamic motion of $e^{i\omega t}$ the following equations of motion characterize the system,

$$\left(\left[K^n\right] + \beta\left[G^n\right] - \omega^2\left[M^n\right]\right)\{\bar{q}^n\} = \{\bar{F}^n\} \tag{36}$$

Using this equation a variety of analyses may be formulated. If β and ω are set equal zero the static analysis is obtained. From the initial stress state thus obtained the geometric stiffness may be calculated. Then by setting $\bar{F}$ and ω to zero the eigenproblem for the buckling parameter β is obtained. Setting $\bar{F}$ to zero and specifying β, the eigenproblem for the vibrational frequencies ω and mode shapes is obtained, taking into account the destabilizing effects of the prestress. If β and ω are specified the forced vibration problem with $\bar{F}$ a function of frequency may be solved. Results of sample cases performed are presented in the next section.

IV Implementation and Results

In order to obtain results from the methodology presented here a computer program, FASOR (Fourier Analysis of Shells of Revolution), has been developed. The program has been designed to minimize core requirements and computer solution time. Through the use of variable dimensioning of all subroutines the amount of core used is exactly the amount needed for a particular problem. Sparse matrix techniques have been employed in most matrix manipulations. Banded matrix techniques have been employed in the static analysis back substitutions and in the sub-space iteration eigensolutions. The sub-space iteration technique [10,11] is very efficient and calculates only the

lowest buckling and vibrational modes desired by the user. (Through the use of frequency shifts it is possible to solve also for either the rigid body modes of the structure, or frequencies in the vicinity of a specified value.)

All analysis paths of FASOR have been checked out and results compared to available closed form and numerical solutions. Since the shell theory employed herein is a third order theory it pertains to thicker shells, i.e. larger thickness to radius ratios, than do most available codes. Unfortunately, scarcity of available solutions for thick shells has so far inhibited the investigation of FASOR's solution accuracy compared to other programs. This and the investigation of the effect of shell bending stresses on stability, which is also unique to FASOR, will be pursued in future studies. In order to make meaningful comparisons, the cases presented in the following are for relatively thin shells ($h/a \sim 0.01$) where correspondence with available solutions will be closest.

Many of the static test cases may be obtained from Timoshenko [12]. The first example is the problem of a semi-infinite circular cylinder with applied end shear, H_o, and moment, M_o. The damped sin-wave solution's results for end radial displacement and rotation for a shell having the following properties:

$a = 10"$, $h = 0.1"$, $E = 30{,}000$ Kips/sq. in., $\nu = 0.3$; are

$$w(0) = .08569\, H_o - .11015\, M_o \qquad (37)$$

$$\beta(0) = -.11015\, H_o + .28318\, M_o$$

Using 9 Type II elements FASOR gives

$$\beta(0) = -.11004 \overset{c}{H}_o + .28303 \overset{o}{M}_o \qquad (38)$$

Using only one Type II element the results are between 8% and 25% in error. Various circular plate bending problems have been used for different harmonics and loading conditions. For these cases displacement results were exact to four digits or more using only one Type II element. The in-plane stiffness of the elements has been checked out using various closed form solutions for conical membrane shells under loading conditions such as internal pressure, symmetric and anti-symmetric weight loading and ring-loads. All results were very accurate using not more than five Type II elements.

A cylinder vibration problem was compared to Forsberg's results [13] using Flügge's cylindrical shell theory. The following dimensions and properties were used: $E = 30\times10^6$ psi, $\nu = 0.32$, $\rho = .000253886$ lb-sec^2/in., $a = 3.045$ in., $h = .06$ in., length = 16.2 in. For classical simply supported boundary conditions $w = v = \overset{s}{N} = \overset{s}{M} = 0$ in wave $n = 4$ Forsberg's lowest frequency is 974 cy/sec. Using 10 Type II elements FASOR gave 973.47 cy/sec.

A comparison for the geometric stiffness effects of the finite element is provided by the buckling problem of a conical frustum loaded by external pressure [14]. The shell investigated has the following properties: $E = 30\times10^6$ psi, $\nu = 0.3$, $h = 0.1$ in., left radius = 5 in., right radius = 10 in., cone angle $\phi = 30^o$, length $2\overset{o}{s} = 10$ in. The boundary conditions are at each

end, $u = w = M_s = N_{s\theta} = 0$. The lowest (critical) buckling pressure was found for circumferential wave n = 9 and is

p_{cr} = 80.53 psi : Ref. 13

p_{cr} = 81.99 psi : 10 Type II elements

p_{cr} = 82.72 psi : 5 Type II elements

p_{cr} = 98. psi : 1 Type II element.

REFERENCES

1. Navaratna, D.R., Pian, T.H.H. and Witmer, E.A., "Stability Analysis of Shells of Revolution by the Finite-Element Method", AIAA Journal, Vol. G, No. 2, February 1968, pp. 355-361.

2. Bushnell, D., "Analysis of Ring-Stiffened Shells of Revolution under Combined Thermal and Mechanical Loadings", AIAA Journal, Vol. 9, No. 3, March 1971, pp. 401-410.

3. Bronowicki, A.J., Nelson, R.B., Felton, L.P. and Schmit, L.A. Jr., "Optimum Design of Ring Stiffened Cylindrical Shells", AIAA Journal, Vol. 13, No. 10, October 1975, pp. 1319-1325.

4. Nelson, R.B., Felton, L.P., and Schmit, L.A. Jr., "Optimum Design of Submerged Cylindrical Shells Subjected to Dynamic Loadings", UCLA-ENG-7587, November 1975.

5. Pappas, M. and Allentuch, A., "Extended Capability for Automated Design of Frame-Stiffened, Submersible, Cylindrical Shells", Computers and Structures, Vol. 4, 1974, pp. 1025-1059.

6. Byrne, Ralph Jr., "Theory of Small Deformation of a Thin Elastic Shell", University of California, Los Angeles, Publications in Mathematics, N.S., Vol. 2, 1944, pp. 103-152.

7. Bolotin, V.V., Nonconservative Problems of the Theory of Elastic Stability, Pergamon Press, New York, 1963.

8. Cohen, Gerald A., "Conservativeness of a Normal Pressure Field Acting on a Shell", AIAA Journal, Vol. 4, No. 10, October 1966, p. 1886.

9. Froberg, C.E., Introduction to Numerical Analysis, 2nd Ed., Addison-Wesley Publishing Co., Reading, Mass., 1969.

10. Dong, S.B., Wolf, J.A., and Petersen, F.E., "On a Direct-Iterative Eigensolution Technique," Int. Jour. for Numerical Methods in Engr., Vol. 4, 1972, pp. 155-162.

11. Bathe, Klaus-Jürgen, Wilson, Edward L., Numerical Methods in Finite Element Analysis, Prentice-Hall, Englewood Cliffs, N.J., 1976.

12. Timoshenko, S. and Woinowsky-Krieger, S., Theory of Plates and Shells, McGraw-Hill, N.Y., 1959.

13. Forsberg, K., "Exact Solution for Natural Frequencies of Ring Stiffened Cylinders," Proceedings of the AIAA/ASME 10th Structures, Structural Dynamics and Materials Conference, New Orleans, LA, April 1969.

14. Baruch, M., Harari, O., and Singer, J., "Influence of In-Plane Boundary Conditions on the Stability of Conical Shells under Hydrostatic Pressure," Israel Journal of Technology, Vol. 5, pp. 12-24, Feb., 1967.

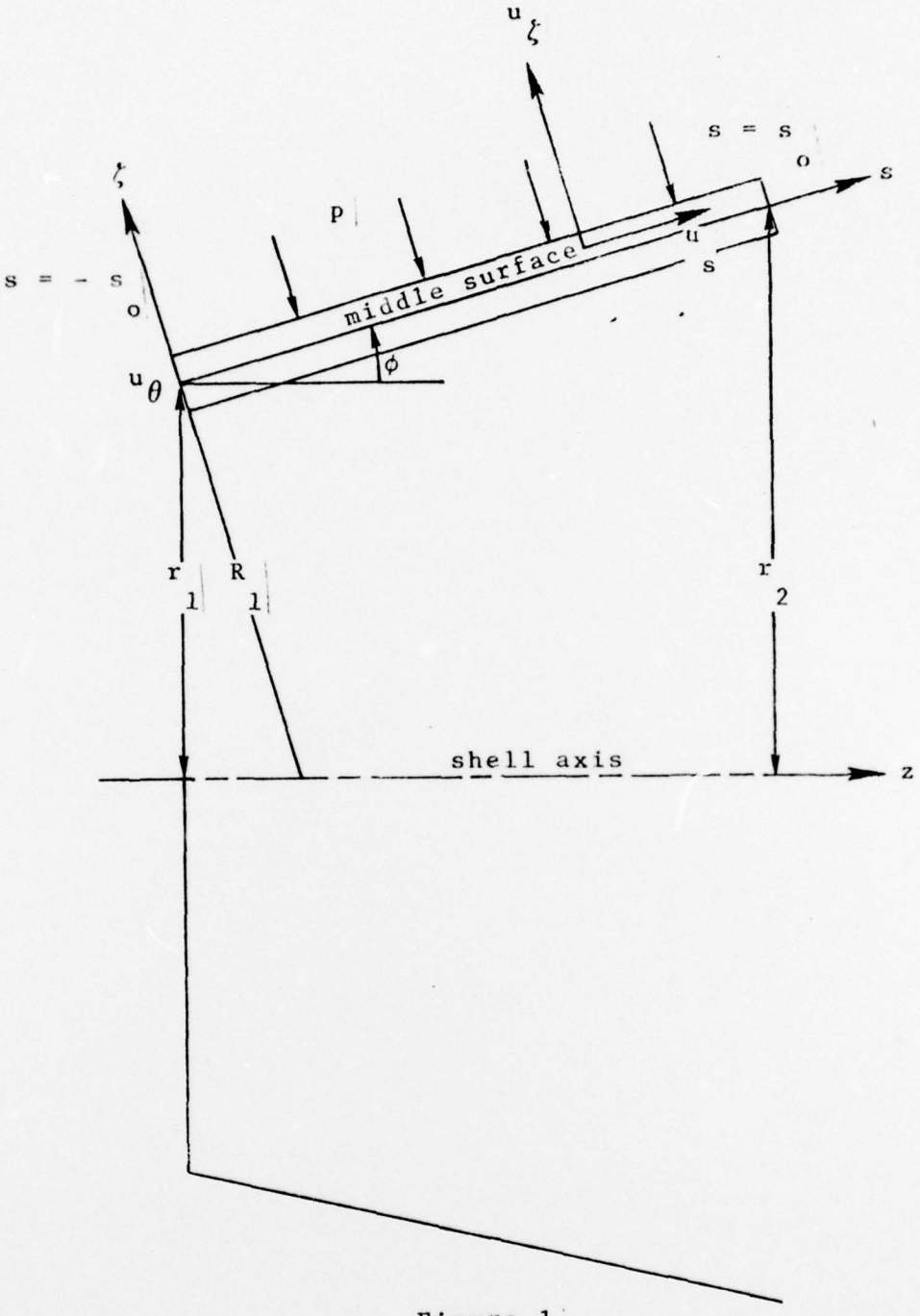

Figure 1

	u	u,s	w	w,s	w,ss	v	v,s
u	ρh			$-\rho \frac{h^3}{12r} \cos\phi$			
u,s							
w			$\rho\left(h + \frac{h^3}{12r^2}\right)$			$\left[-\rho \frac{nh^3}{6r^2} \cos\phi\right]$	
w,s				$\rho \frac{h^3}{12}$			
w,ss			Symmetric				
v						$\rho\left(h + \frac{h^3}{4r^2} \cos^2\phi\right)$	
v,s							

Figure 3. Matrix $\left[\tilde{M}_n\right]$.

$\frac{1}{r}\left(N_\theta^e - M_\theta^e \frac{\cos\phi}{r}\right)\cdot\left(\sin^2\phi + n^2\right)$		$\frac{1}{r^2}\sin\phi\cos\phi N_\theta^e + M_\theta^e \frac{\cos\phi}{r^3}\left(-\cos\phi\sin\phi + 2\frac{\sin\phi}{\cos\phi}n^2\right) + p\frac{\sin\phi}{r}$	$-\left(\sin^2\phi + n^2\right)\frac{M_\theta^e}{r^2}$		$-2n\frac{\sin\phi}{r^2}N_\theta^e$	
	N_s^e	p^e		$-M_s^e$		
		$\frac{N_\theta^e}{2}(\cos^2\phi + n^2) + M_\theta^e\frac{\cos\phi}{r^3}(3n^2 - \cos^2\phi) + \frac{p^e\cos\phi}{r}$	$-\frac{\cos\phi\sin\phi}{r^2}M_\theta^e$		$-2n\frac{\cos\phi}{r^2}N_\theta^e - \frac{(n^3 - n)}{r^3}M_\theta^e - p^e n/r$	$n\frac{\sin\phi}{r^2}M_s^e$
			N_s^e			$-n\frac{M_s^e}{r}$
	Symmetric					
					$\frac{1}{r^2}\left(1+n^2\right)\left(N_\theta^e + \frac{\cos\phi}{r}M_\theta^e\right) + \frac{p^e\cos\phi}{r}$	$-\frac{\cos\phi\sin\phi}{r^2}M_s^e$
						$\frac{N_s^e + 2\cos\phi M_s^e}{r}$

Figure 4. Matrix $\left[\tilde{C}_n\right]$.

$\frac{\sin^2\phi}{2}\left(D+K\frac{\cos^2\phi}{2}\right)$ $+ D\frac{(1-\nu)}{2}n^2$ $2r$	$D\nu\frac{\sin\phi}{r}$	$\frac{\cos\phi\sin\phi}{2}\cdot\left(D+K\cdot\right.$ $\left.\cdot\frac{\cos^2\phi}{2} - \frac{K(3-\nu)n^2}{2}\right)$ $r \quad 2r$	$\frac{K\cos\phi}{3}\cdot$ $\cdot\left(\sin^2\phi+\frac{(1-\nu)}{2}n^2\right)$	0	$-D\frac{(3-\nu)}{2}\frac{\sin\phi}{2}n +$ $K\frac{\cos^2\phi\sin\phi}{4}(1-\nu)n$	$\frac{n}{r}\frac{(1-\nu)}{2}\cdot$ $\cdot\left(D-K\frac{\cos^2\phi}{2}\right)$
	D	$D\nu\frac{\cos\phi}{2}$	0	$-K\frac{\cos\phi}{r}$		0
		$\frac{K}{4}\left[\left(n^2-\cos^2\phi\right)^2+2(1-\nu)\cdot\right.$ $\left.\cdot\sin^2\phi n^2\right]+D\frac{\cos^2\phi}{2}$	$K\frac{\sin\phi}{3}\cdot$ $\cdot\left(\cos^2\phi-(3-2\nu)n^2\right)$	$-k\nu\frac{n^2}{2}$	$-\cos\phi\frac{n}{2}\cdot\left(D+\right.$ $\left.\frac{3K(1-\nu)}{2}\frac{\sin^2\phi}{2}\right)$	$\frac{3K(1-\nu)}{2}\cdot$ $\cdot\cos\phi\sin\phi\frac{n}{3}$
			$K\frac{\sin^2\phi}{2}$ $+ 2K(1-\nu)\frac{n^2}{3}$	$K\nu\frac{\sin\phi}{r}$	$\frac{3K(1-\nu)}{3}\cdot$ $\cdot\cos\phi\sin\phi\cdot n$	$-\frac{3K(1-\nu)}{2}\cdot\frac{\cos\phi}{2}\cdot n$
				K	$K\nu\frac{\cos\phi}{2}$	0
		Symmetric			$\frac{D}{2}\left(n^2+\frac{(1-\nu)}{2}\sin^2\phi\right)$ $+ K\frac{(1-\nu)}{4}\cdot$ $\cdot\cos^2\phi\sin^2\phi$	$-(1-\nu)\frac{\sin\phi}{r}\cdot$ $\cdot\left(\frac{D}{2}+K\frac{\cos^2\phi}{2}\right)$
						$\frac{D(1-\nu)}{2}+$ $+ K\frac{\cos^2\phi}{2}(1-\nu)$

Figure 2. Matrix $\left[\tilde{K}\,n\right]$.

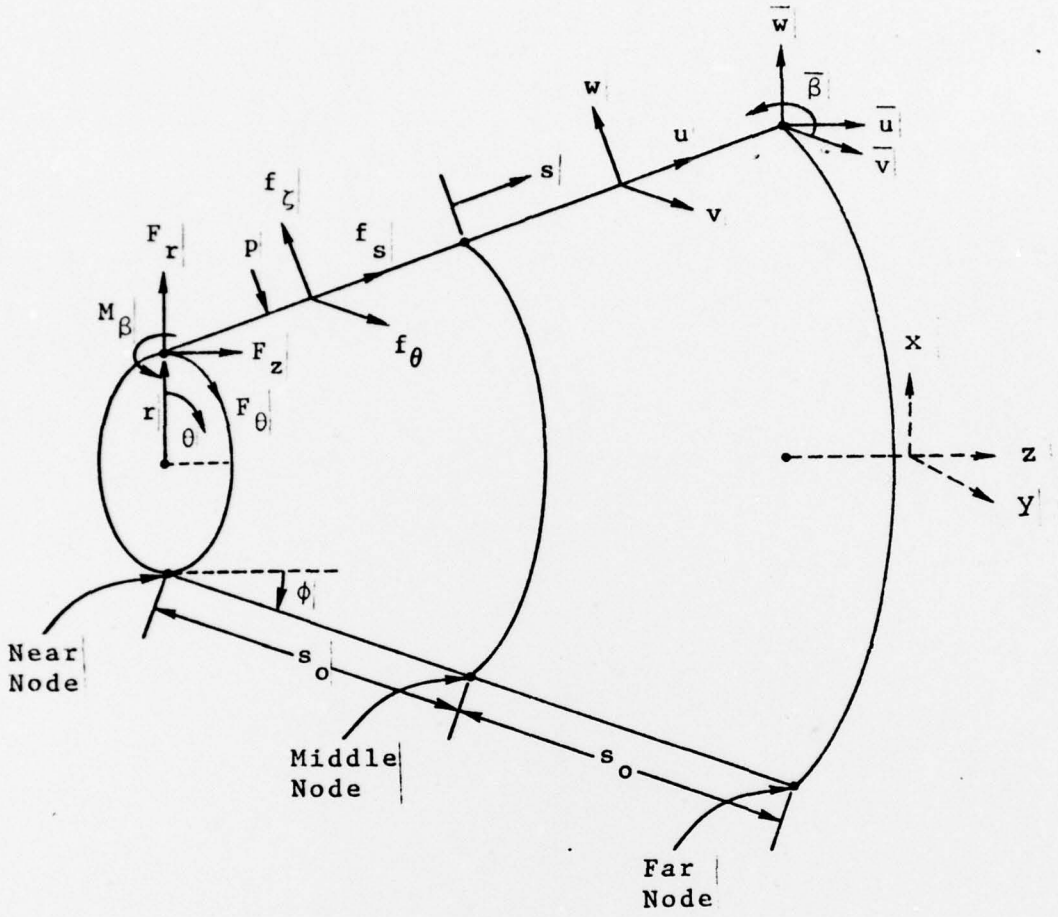

Figure 5. Conical Frustum Element.